Experimental Transition Investigation of a Free-Shear Layer Above a Cavity at Mach 3.5

Rudolph A. King,* Theodore R. Creel Jr.,* and Dennis M. Bushnell†
NASA Langley Research Center, Hampton, Virginia 23665

The transition behavior of a free-shear layer above a cavity with high and low levels of freestream acoustic disturbances has been investigated at Mach 3.5. Optical, mean pitot pressure, and hot-wire techniques were used to detect transition locations. The transition Reynolds numbers obtained were between Re_{T_r} = 363,000 and 530,000, in good agreement with previous (conventional, high noise facility) results. The study indicated that the effects of lowering freestream noise on Re_{T_r} were minimal but, as expected, favorable (higher Re_{T_r}). However, hot-wire anemometry indicated that the shear layer disturbance growth differed considerably for high and low noise levels. Also, the growth frequencies are considerably below expectations from linear stability theory. Correlations between hot-film sensors mounted on the cavity floor indicated the presence of disturbances, believed to be vorticity and/or entropy waves, convecting upstream at about 7.2–11.5% of the freestream velocity. Upstream convected disturbances (acoustic as well as the vorticity/entropy waves indicated herein) are believed to be at least partially responsible for the insensitivity of Re_{T_r} to the freestream acoustic disturbance field.

Nomenclature

a = sonic velocity
e = fluctuating voltage
f = frequency
M = Mach number
P = pressure
P_b = base pressure
P_s = surface pressure
P_t = pitot probe pressure
$R_{AB}(\tau)$ = space-time correlation coefficient, $\overline{e_A(t)e_B(t+\tau)}/e'_A e'_B$
Re = unit Reynolds number, U_1/ν_1
Re_{T_r} = transition Reynolds number, $U_1 X_{T_r}/\nu_1$
T = temperature
U = velocity
U_R = reverse velocity
X = distance from model step, see Fig. 1
Y = distance from forward portion of model surface, see Fig. 1
$-\alpha_i$ = spatial amplification growth rate
γ = ratio of specific heats
δ = shear layer thickness
θ_w = wedge angle
λ = nondimensional velocity ratio, $(U_1 - U_2)/(U_1 + U_2)$
ν = kinematic viscosity
ξ = distance from nozzle throat
τ = time delay

Subscripts and Superscripts

∞ = tunnel freestream conditions
0 = tunnel stagnation conditions, initial shear layer value
1,2 = properties on high and low velocity side, respectively
A,B = film numbers 0, 1, 2, . . . , 9
c = convective properties
e = edge properties
L = conditions at reattachment
Tr = conditions at transition
$'$ = rms values
$-$ = time-averaged values

Introduction

RENEWED interest in air-breathing hypersonic flight has refocused attention on supersonic combustion ramjet (scramjet) engine performance and particularly on the central issue of the streamwise length required to efficiently mix and burn the fuel/air mixture at high Mach numbers. This is especially critical at high Mach numbers, where near-axial injection is required for fuel-addition thrust recovery. To achieve efficient combustion, micro- (molecular) mixing *and* the mixing associated with the exchange of momentum by large-scale motions are needed between the fuel and air streams. This problem has generated considerable research, both experimental and theoretical, to understand the physics associated with compressible free-mixing flows and enhance scramjet combustor efficiency.

A fundamental requirement for efficient mixing is transition to turbulent flow within the mixing zones. The conventional two-dimensional free-shear layer transition process entails a short linear region followed by an extensive nonlinear portion initially composed (predominately) of large-scale vortices induced by the Kelvin-Helmholtz instability. These large-scale, coherent structures have been observed experimentally by Matsuo et al.,[1] Papamoschou and Roshko,[2] and others.

The "convective Mach number" and its relationship to free-mixing flows were investigated by Papamoschou and Roshko[2] and Bogdanoff.[3] The convective Mach number M_c is defined as the Mach number referenced to a frame moving with a convective velocity U_c of the dominant waves and structures in the shear layer. For turbulent compressible mixing layers, mixing chracteristics have been experimentally investigated by Papamoschou and Roshko,[2] Bogdanoff,[3] Ikawa and Kubota,[4] and others; all these researchers concluded that an increase in compressibility (convective Mach number) can have adverse effects on mixing (reduced growth rates). In

Presented as Paper 89-1813 at the AIAA 20th Fluid Dynamics, Plasma Dynamics and Lasers Conference, Buffalo, NY, June 12–14, 1989; received Sept. 15, 1989; revision received June 4, 1990; accepted for publication Sept. 23, 1990.

*Aerospace Engineer, Experimental Flow Physics Branch, Fluid Mechanics Division. Member AIAA.
†Associate Chief, Fluid Mechanics Division. Fellow AIAA.

particular, Samimy and Elliott[5] indicated that as the convective Mach number increases, the coherency of the large-scale structures in the supersonic side of the mixing layer decreases. This is believed to limit the lateral transport of kinetic energy and also the entrainment of the flow on the supersonic side, which in turn decreases the growth rate.

Linear stability calculations by Ragab and Wu[6] and Gropengiesser[7] for two-dimensional free-shear layers (with no adjacent surfaces) indicate that an increase in Mach number from $M_1 = 0$ to 3 has a stabilizing effect. Recent numerical solutions of Balsa and Goldstein[8] indicate that the most unstable waves are skewed for the higher Mach number shear layer case in agreement with Refs. 7 and 9. Earlier, Chapman et al.[10] showed experimentally that an increase in Mach number from $M_1 = 0.5$ to 3.5 resulted in almost an order of magnitude increase in Re_{T_θ}. Gilreath and Schetz[11] experimentally and analytically investigated free-shear layers induced by supersonic and subsonic tangential surface injection for freestream Mach numbers of 2.85 and 4.19. They found that an increase in stability occurred with either a decrease in the injectant Mach number or an increase in the external flow Mach number. Similar experimental results have been obtained in Refs. 12 and 13.

The stability calculations in Refs. 6 and 7 did not consider the presence of an adjacent surface with an intervening flow. The effects of an adjacent surface (but with attached flow) on the stability of two-dimensional free-shear layers have been studied by Tam and Hu,[14] Mack,[15] and Macaraeg and Streett.[16] They found that new supersonic instabilities, as opposed to the Kelvin-Helmholtz instability, are dominant at high supersonic convective Mach numbers for confined free-shear flows. The coupling of the unsteady motion of the shear layer and reflections of acoustic waves by the adjacent surfaces is believed to produce these new instability waves.

Available compressible free-shear layer (experimental) transition information is "sketchy" at best and limited to data taken in conventional wind tunnels with high freestream acoustic disturbance levels generated by turbulent boundary layers on the nozzle walls. The purpose of the present study was to use the unique capability of the Supersonic Low-Disturbance Pilot Wind Tunnel[17] to experimentally evaluate the effect of freestream acoustic disturbances on transition for a particular (and commonly studied) free-shear layer, the cavity flow case. Actual scramjet combustor flows exhibit several destabilizing features such as three-dimensional mean flows, adverse pressure gradients, chemical reactions, and interacting (unsteady) shock waves that are not included in the present data.

Apparatus and Test Conditions

Facility

The study was conducted using the Mach 3.5 two-dimensional nozzle in the Supersonic Low-Disturbance Pilot Wind Tunnel located at the Langley Research Center. This tunnel provides a low noise test region in the upstream part of the uniform flow test rhombus when the nozzle-wall boundary layers at the "acoustic origin" locations are laminar. The laminar nozzle-wall boundary-layer conditions were achieved by removing the boundary layer just upstream of the nozzle throat. A complete description of the tunnel and the effects of wall-radiated acoustic noise on boundary-layer transition are given by Beckwith et al.[17]

Model

The model tested was a backward-facing step, bottom plate-wedge combination (see Fig. 1). The relative model location for Phase II (Phase II will be discussed in the next section) within the quiet test rhombus of the nozzle is also shown in the figure. The forward portion of the model was a 15 deg half-wedge with a 15.2 × 15.2-cm square (6 × 6 in.) planform area. The flat surface of the half-wedge had an excellent surface finish with a rms value of 0.10 (4) to 0.15 μin. (6 μin.); this avoided tripping the attached boundary layer to ensure a laminar separated shear layer. The backward-facing step height was fixed at 0.81 cm (0.32 in.). The bottom plate was 22.9 cm (9 in.) long with a 15.2-cm (6 in.) span. The model was equipped with two pressure taps to monitor the pressures across the separated shear layer, one on the flat surface 0.51 cm (0.20 in.) upstream of the step and the other on the vertical face of the backward-facing step 0.30 cm (0.12 in.) above the bottom plate. The bottom plate (cavity floor) was equipped with 10 hot-film sensors spaced equally in the streamwise direction at 0.64 cm (0.25 in.). The sensors were placed 0.64 cm (0.25 in.) off the centerline of the model. The first and last sensors were located at $X = 1.91$ (0.75) and 7.62 cm (3 in.) downstream of the backward-facing step, respectively.

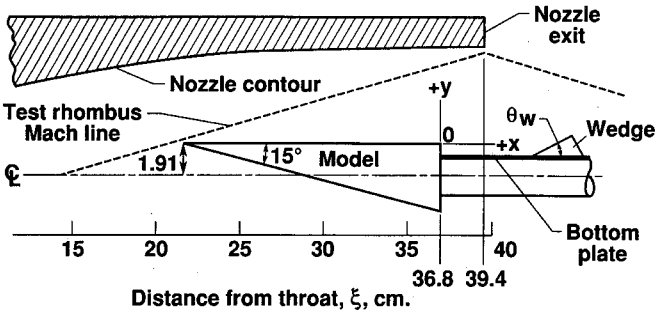

Fig. 1 Model location (for phase II) in nozzle test rhombus.

The variable-angle wedge located downstream of the step on the bottom plate was used to balance the pressures on both sides of the separated shear layer following the technique of Hayakawa et al.[18] By adjusting the wedge angle θ_w from 10 to 30 deg and its location from $X = 12.38$ (4.875) to 22.9 cm (9 in.) downstream of the step, the base pressure and surface pressure could be balanced for all test conditions to within 2.5%,

$$\frac{|P_b - P_s|}{P_s} < 0.025.$$

Instrumentation and Test Conditions

The present research was conducted in two phases. The purpose of phase I was to detect optically free-shear layer transition with and without laminar nozzle wall boundary layers for a range of Re. The schlieren tests were conducted with the model step located as far forward as 3.81 cm (1.5 in.) upstream and as far back as 7.62 cm (3 in.) downstream of the nozzle-exit plane. The separated shear layer was observed using the schlieren system. Schlieren photographs were taken with an exposure time of 10 μs at various Re_∞.

The range in Re_∞ was obtained by varying the tunnel stagnation pressure, and the angle and/or location of the wedge mounted on the bottom plate (see Fig. 1) were varied to maintain the balanced static pressure condition. For each model configuration and tunnel wall condition (laminar or turbulent), there was a unique Re_∞ required to balance the pressures across the shear layer. Increasing the wedge angle and/or moving the wedge upstream required an increase in Re_∞ for balanced conditions. The base and surface pressures were balanced to within 1.5% in this phase.

Phase II was a more detailed study in which mean and dynamic flow effects in the shear layer were investigated. These tests were conducted with the model step located 2.54 cm (1 in.) upstream of the nozzle-exit plane. The angle of the downstream wedge was $\theta_w = 25$ deg, and its location was $X = 12.38$ cm (4.875 in.) from the step.

Mean pitot pressure data were taken to map the mean flowfield and to detect transition location. A streamlined pitot probe (frontal dimensions of 0.25 mm [0.01 in.] by 0.64 mm

[0.025 in.]) was used to minimize flow interference. Surveys were taken across the shear layer in the Y direction in increments of 0.25 mm (0.01 in.) at selected X locations along the centerline of the model.

A constant curent hot-wire anemometer was employed to estimate transition locations and investigate the disturbance growth in the free-shear layer. The dynamic response of the instrumentation was limited to about f = 200 kHz. Again a streamlined probe was used to minimize interference. The spacing of the wire supports was 0.51 mm (0.02 in.). Tungsten wires with diameters of 0.0025 mm (0.00010 in.) and 0.0030 mm (0.00012 in.) were used. Surveys were again taken across the shear layer in the Y direction in increments of 0.51 mm (0.020 in.) at selected X locations along the centerline of the model. Constant temperature hot-film anemometers were employed to simultaneously map wall region fluctuations in the subsonic recirculating zone. The output signals were digitized using a multichannel A/D converter. A sample rate of 200 kHz and a record length of 0.33 s were used. The dynamic response of the instrumentation was limited to about 10 kHz.

The freestream test conditions for phase I were M_∞ = 3.5, T_o = 21 (70) to 24°C (75°F), and Re_∞ = 23,622 (60,000) to 59,055/cm (150,000/in.). The test conditions for phase II were M_∞ = 3.5, T_o = 21 to 24°C, and Re_∞ = 57,087 (145,000) and 43,307/cm (110,000/in.) for the cases of laminar and turbulent wall conditions, respectively.

Freestream Hot-Wire Measurements

In conventional wind tunnels for $M_\infty \geq 3$, the dominant source of freestream disturbances is the acoustic radiation from eddies in the turbulent boundary layers on the nozzle walls.[19-21] This is unlike the low-speed case where vorticity disturbances dominate. As a result, disturbances in the freestream are referred to herein as freestream acoustic disturbances. To check the quality of flow within the tunnel, freestream rms fluctuating pressure $(P'_\infty/\overline{P}_\infty)$ data (Fig. 2), as determined from hot-wire surveys with laminar and turbulent nozzle wall boundary layers, were obtained. The $(P'_\infty/\overline{P}_\infty)$ data were obtained directly from a mode diagram analysis.[22] These surveys were taken 2.54 cm (1 in.) above the nozzle centerline at distances from the nozzle throat of ξ = 29.21 cm (11.5 in.) to 49.53 cm (19.5 in.). The surveys covered the approximate location occupied by the model during the tests. The data of Fig. 2 indicate an order of magnitude change between laminar and turbulent nozzle-wall conditions. These results compare favorably with the data of Figs. 5 and 6 from Ref. 17.

Freestream power spectra of the hot-wire signals[23] for turbulent nozzle-wall boundary layers indicate wideband energy levels (200 Hz $< f <$ 60 kHz). For the laminar wall condition, freestream power spectra indicate no detectable differences between the measured signal and instrument noise.

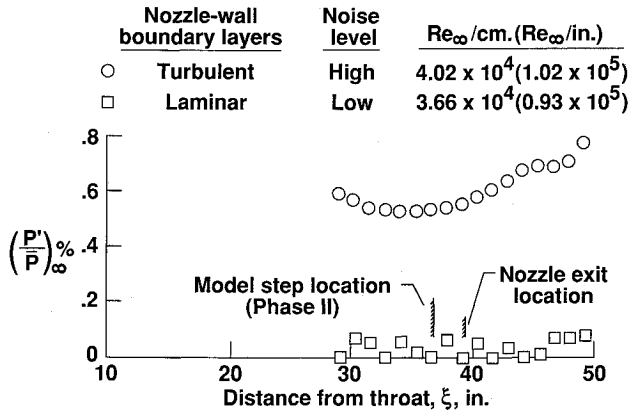

Fig. 2 Freestream rms fluctuating pressures for M_∞ = 3.5.

Results and Discussion

Transition Location

1. Visualization Data

The separated shear layer was the main interest of the study. As stated previously, the objective of phase I was to detect optically transition location. Figure 3 shows a typical schlieren photograph where a sketch of the upstream portion of the model is included for clarity. The most important parts of the flowfield are also identified in the figure. Because the static pressure was balanced across the shear layer, the boundary layer separated from the model surface free of any measurable expansion and/or compression regions usually associated with similar flows.[24] The nozzle-exit shock (Fig. 3) was found not to affect the transition location, provided the transition location was well upstream of the intersection of the nozzle-exit shock and shear layer.

The thin, well-defined part of the shear layer in the figure represents the laminar flow. A relatively rapid increase in shear-layer mean growth rate was used as the transition criterion (as in most previous high-speed shear-layer transition studies). The approximate transition location is indicated by the arrow in the figure. No attempt was made to differentiate between the onset and end of transition.

Transition Reynolds number Re_{T_r} as a function of Re for the present experiment is shown in Fig. 4. The unfilled symbols represent data obtained from schlieren photographs. The circles and squares in the figure represent high and low noise levels, respectively. The Re_{T_r} values obtained were between 400,000 and 530,000 where X_{T_r} was measured from the backward-facing step. As is evident from the figure, the effects of lowering the freestream acoustic disturbance levels on Re_{T_r} are minimal, but the data indicate a slightly higher value (25%) of Re_{T_r} at the highest Re under low-noise conditions. Also, there is very little Re effect on Re_{T_r}. It should be noted that the optical technique and the ambiguity of start vs end of transition will likely introduce "scatter" into the data on

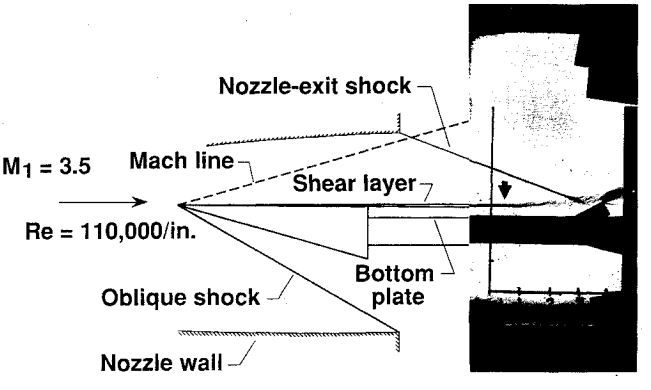

Fig. 3 Schlieren photograph of free-shear layer; M_∞ = 3.5 (scale in inches).

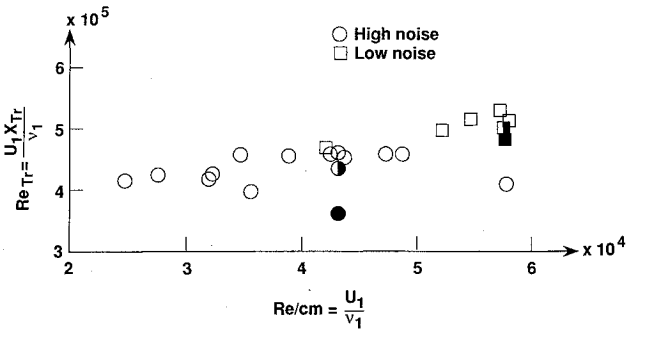

Fig. 4 Transition Reynolds number vs unit Reynolds number; M_∞ = 3.5 (unfilled symbols represent schlieren data; half-filled symbols, mean pitot pressure data; and filled symbols, hot-wire data).

the order of the differences noted. The half-filled and filled symbols in Fig. 4 will be discussed in the following sections.

2. Mean Profile Data

Mean pitot pressure data were taken to map the mean flowfield in the shear layer and to detect transition location (phase II of the study). For this configuration, the nozzle-exit shock intersected the shear layer approximately 2.54 cm downstream of the wedge; as a result, the shock had no direct influence on the shear layer. Figure 5 shows some typical normalized pressure profiles P_t/P_0 at the indicated X locations for the high-noise case. The initial shear-layer thicknesses are approximately δ_0 = 1.83 mm (0.072 in.) and 1.78 mm (0.070 in.) based on $0.9U_1$ for Re_∞ = 43,307 (high noise) and 57,087/cm (low noise), respectively. The pressure profiles indicate that the shear-layer growth on the high velocity side (U_1 = 651 m/s [2,135 ft/s]) is significantly less than the growth on the low velocity side ($U_2/U_1 \ll 1$).

A rapid increase in the shear-layer growth rate deflected the local external flow outward. As a result of the flow deflection, compression waves, which are visible in the schlieren photographs, were formed on the supersonic side of the shear layer. This resulted in a decrease of M_e in the vicinity of the transition location. A decrease in Me is associated with an increase in the local edge P_t. This is clearly evident in Fig. 5. The approximate transition location was taken as the first X station where a significant increase in the local edge P_t/P_0 was observed. For the case with high noise level, the transition location was approximately X_{Tr} = 10.16 cm (4 in.), which implies Re_{T_r} = 440,000 (see Fig. 5). Similarly for the case with low noise level, the transition location was approximately X_{Tr} = 8.89 cm (3.5 in.), which implies Re_{T_r} = 510,000. Again, it is obvious that there were no first-order effects of the freestream acoustic field on Re_{T_r}. The aforementioned data are included in Fig. 4 and are represented by the half-filled symbols. The previous Re_{T_r} values are in good agreement with the Re_{T_r} values obtained from schlieren photographs indicating that 1) the optical technique is relatively accurate, and 2) the nozzle-exit wave system had no direct effect on the transition location.

3. Hot-Wire Data

Hot-wire surveys were taken across the shear layer in the Y direction, -2.54 mm (-0.1 in.) $< Y <$ 2.54 mm (0.1 in.), in increments of 0.51 mm (0.020 in.) at selected X locations (typically, every 1.27 cm [1/2 in.]). Root-mean-square values of the fluctuating voltage e' were obtained at each survey station. As the probe traversed the shear layer, the output signal increased to a maximum at a point inside the shear layer. A plot of the maximum e' values as a function of X is given in Fig. 6. For both high and low freestream noise levels, there was a significant increase in the slope of e'_{max} vs X, which is indicative of the onset of transition (power spectra results will be discussed later). Straight line fairings of the laminar and transitional data are also shown in the figure. The onset of transition was taken to be the intersection of these faired lines and is indicated by the arrows in the figure.

The previous data are also included in Fig. 4 and are represented by the filled symbols. The Re_{T_r} measured by the hot wire for the high-noise case is somewhat lower (~20%) than the Re_{T_r} measured by the schlieren and mean pitot pressure techniques at the same Re. The hot-wire detection method is more sensitive to transition onset than the other two methods. One speculation may be that the extent of transition for the high-noise case is longer than that for the low-noise case. However, insufficient data exist to make such a conclusion. The probe interference may have also contributed to the lower value of Re_{T_r}.

4. Comparison with Previous Results

In contrast with the present study, previous results[25] for lower values of λ ($\lambda \simeq 1$ for the present study) with two supersonic streams indicated a large influence of the facility disturbance field, as inferred from the observed sensitivity to

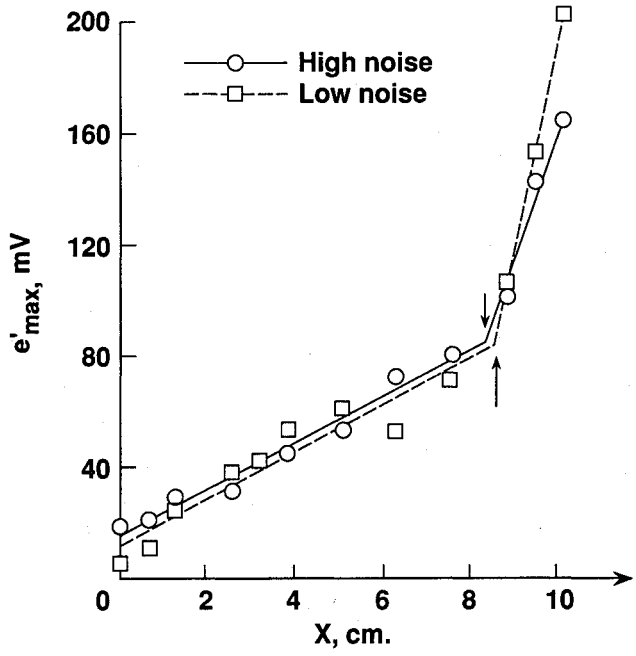

Fig. 6 Maximum (measured) hot-wire response across shear layer.

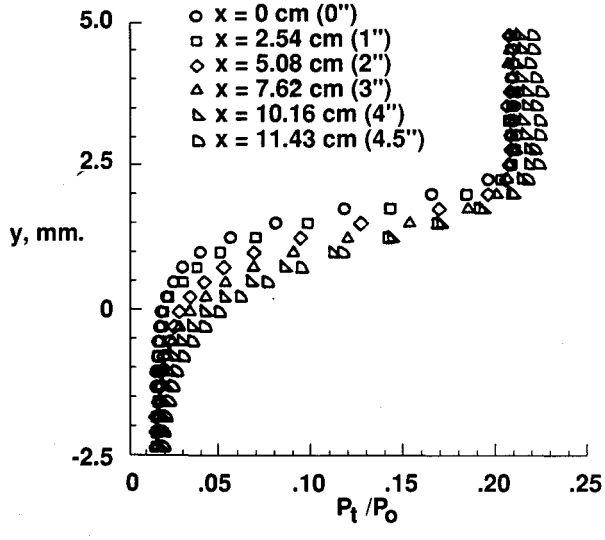

Fig. 5 Shear-layer pitot pressure profiles; M_∞ = 3.5, Re_∞ = 4.33 × 10⁴/cm (1.10 × 10⁵/in.), high $(P'/\bar{P})_\infty$.

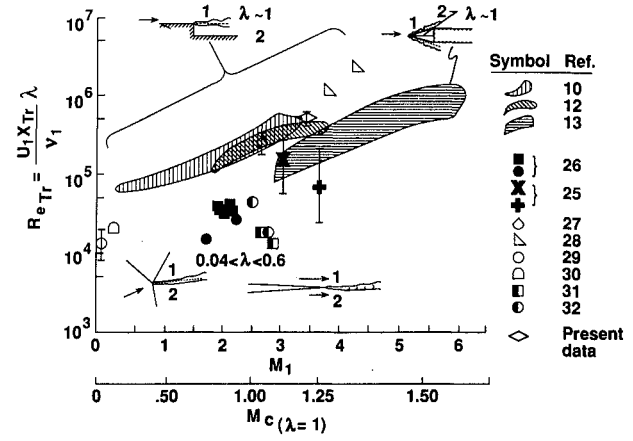

Fig. 7 Transition Reynolds number vs Mach number on the high velocity side.

Re. Figure 23 of Ref. 25 indicates that, for small λ values, the Re_{T_r} increased almost an order of magnitude for a Re range of 39,370 (100,000) to 196,850/cm (500,000/in.).

Available free-shear layer transition data[10,12,13,25-32] for $T_{01} \simeq T_{02}$ in the form of Re_{T_r} as a function of M_1 is presented in Fig. 7. The lower scale corresponds to the convective Mach number,

$$M_{c(\lambda=1)} = \frac{M_1}{1 + (1 + M_1^2/5)^{1/2}}$$

as defined by Papamoschou and Roshko[2] for the case where $\gamma_1 = \gamma_2 = 1.4$, $\lambda = 1$, and $T_{01} = T_{02}$. All of the data were obtained in conventional (noisy) wind tunnels except for the present data. Note that the Re_{T_r} is scaled by λ. This scaling was suggested by Edney[33] in an attempt to take into account the first-order effects of the velocity difference across the shear layer. The data were obtained from free-shear layers generated by a variety of geometries.

The transition data on the upper half of the figure were obtained (as in the present case) from separated flows. The geometries include two-dimensional forward[10] and backward-facing steps,[10,29] axisymmetric backward-facing steps,[27,28] two-dimensional (present data, in excellent agreement with the previous results) and axisymmetric[12] cavities, and axisymmetric spiked-nose bodies.[13] These free-shear flows have a finite initial shear-layer thickness ($\delta_0 \neq 0$), except for the shear layer generated from the axisymmetric spiked-nose body where $\delta_0 \simeq 0$. In addition, there is 1) an intervening *subsonic recirculating* zone, and 2) a *nearby surface*. The high values of λ, $\lambda \simeq 1$ ($U_2/U_1 << 1$), are associated with high M_c values for a given M_1.

The filled symbols in the figure were obtained from shear layers generated by shock-on-shock interactions.[25,26] These flows have a zero initial shear-layer thickness, $\delta_0 \simeq 0$, and no trailing-edge effects. There is also no recirculating flow or nearby surfaces. The λ values are fairly small, $0.04 < \lambda < 0.592$, and correspond to low M_c values for a given M_1. These data may be particularly susceptible to freestream acoustic effects due to the possible conversion, via shock motion, of acoustic energy into vorticity.

The remaining set of data in the figure (half-filled symbols) were obtained from shear layers generated by splitter plates and nozzle exits.[31,32] The nonzero δ_0 values correspond to an initial vorticity distribution field in the shear layer. These shear layers have no recirculating regions and no nearby surfaces in the flowfield. The λ values can range from high to low values, which implies high to low M_c values for a given M_1, respectively.

There is considerable spread in the Re_{T_r} data shown in Fig. 7. Simply scaling Re_{T_r} by λ may be inadequate for the scope of shear-layer transition data shown. Reference 6 indicates that there is a complex relationship between the maximum $-\alpha_i$ and λ for compressible free-shear flows, unlike the simple linear relationship for incompressible free-shear flows. Also, the transition data were obtained from shear layers with different initial conditions. The initial disturbance fields of the geometries with the trailing-edge effects are acoustic radiation from nozzle walls, whereas for the shear layers generated from shock-on-shock interaction, the disturbance fields may have been due primarily to shock unsteadiness. This, in conjunction with the fact that each geometry had its own mean-flow profiles (two-dimensional and axisymmetric), which are functions of λ and M_c, results in different stability characteristics for each shear layer.

According to linear stability calculations[7] for $\lambda = 1$, there is a rapid decrease in $-\alpha_i$ around $M_1 \simeq 1.5$ ($M_c \simeq 0.7$). As a result, one would expect the shear layers generated from separated flows ($\lambda \simeq 1$) to have a marked increase in Re_{T_r} (because of the rapid decrease in $-\alpha_i$) around $M_1 = 1.5$. However, according to Fig. 7, this is evidently not the case. Speculations on this will be addressed later.

Disturbance Field

1. Hot-Wire Data

Hot-wire data were acquired, for both high and low freestream disturbance fields, to map the shear-layer disturbance growth. Some typical power spectra of the hot-wire signals are shown in Figs. 8 and 9. Note that the instrument noise was subtracted from the actual hot-wire signal in these power spectra. As stated earlier, the dynamic response of the hot-wire system was limited to about $f = 200$ kHz; however, the signals obtained in the shear layer were at $f < 100$ kHz. The figures show a series of power spectra for cases with high and low freestream noise levels at $Y = 2.54$ (0.1), 1.02 (0.04), and -2.54 mm (-0.1 in.) at selected X locations. At $Y = 2.54$ mm, the probe was located close to the edge of the shear layer (on the high velocity side). For both high (Fig. 8a) and low (Fig. 9a) freestream noise levels, significantly higher freestream energy levels (near the edge of shear layer) for $X > 5.08$ cm (2 in.) were observed as compared to the energy levels measured without the shear layer model.[23] This increase in energy was presumably due to the presence of the shear layer.

The maximum hot-wire response detected across the shear layer was usually around $Y = 1.02$ mm (Figs. 8b and 9b). Note that the ordinate for these plots is 2×10^{-8}, two orders of magnitude higher than the ordinate for the other plots. It is interesting to note the dissimilarity in the dynamic response of the shear layer between the cases with high and low freestream disturbance levels (Figs. 8b and 9b). For the high-noise case (Fig. 8b), the large peaks at $f \simeq 16$ kHz may have resulted from an interaction between the freestream wideband disturbances with the shear layer dynamic flowfield. Note that a significant amount of the shear layer energy occurred at $f \simeq 16$–18 kHz. For the low-noise case (see Fig. 9b), there appeared to be no single, narrow-band disturbances present. Upstream of transition, only low-frequency ($f < 10$ kHz) signals appeared in the spectra. Note that in both Figs. 8b and 9b, there was significant broadening in the power spectra as the distance X increased in agreement with the estimated transition location of Fig. 6. This is attributed to transitional flow.

Figures 8c and 9c show power spectra plots at $Y = -2.54$ mm. At this location, the probe was near the edge of the shear layer on the low-velocity side. These spectra are different in some ways to those at $Y = 1.02$ mm. For the high-noise case (see Fig. 8c), only low-frequency ($f < 8$ kHz) fluctuations showed up in the spectra for $X < 7.62$ cm (3 in.). However, at $X > 8.89$ cm (3.5 in.), the energy peaks at $f \simeq 16$ kHz became visible. For the low-noise case (Fig. 9c), there was significant low-frequency ($f < 10$ kHz) energy present for $X < 7.62$ cm whereas for $X > 7.62$ cm there was significant broadening in the spectra.

2. Hot-Film Data

Because of the apparent insensitivity of the Re_{T_r} to the freestream disturbance field, 10 hot-film sensors were placed along the cavity floor (as described previously) to measure the disturbance field in the subsonic recirculating zone. The main objective of this part of the study was to determine whether any upstream convecting disturbances were present in this region. The sensors were labeled 0 through 9, where sensors 0 and 9 were located at $X = 1.91$ (0.75) and 7.62 cm (3 in.), respectively. Ten constant temperature hot-film anemometers were used to power the films.[34]

Two-point correlations, $R_{AB}(\tau)$, were obtained between different sensors to track any disturbances in the recirculating zone. Note that the time delay τ is in the signal of sensor B. Figure 10 shows a plot of $R_{AB}(\tau)$ referenced to sensor 9 for the low-noise case. As expected, the correlation between sensors 9 and 8, R_{98}, was higher than R_{97}, R_{96}, etc. The corresponding plot for the high-noise case is very similar to the one shown. The correlations between adjacent sensors are

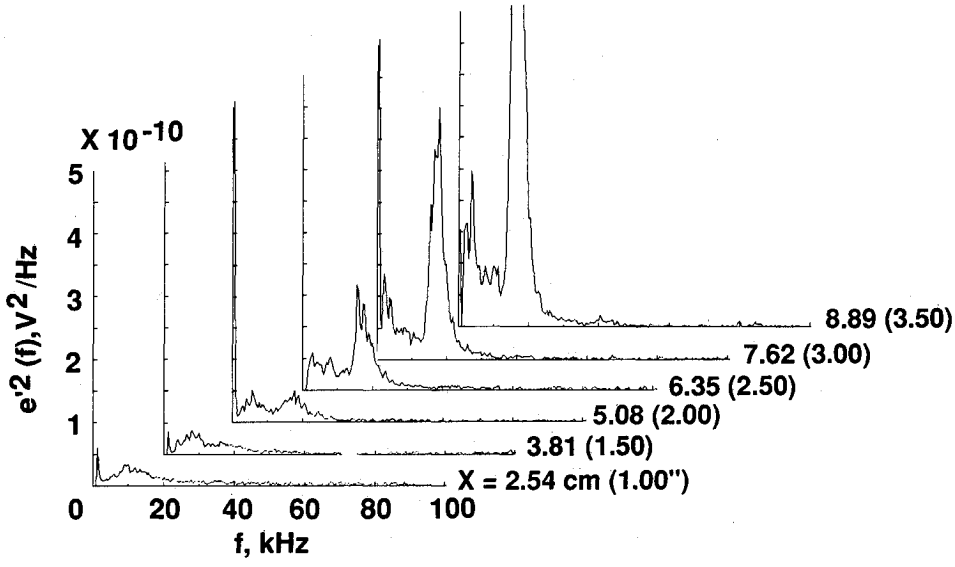

a) Y = 2.54 mm (0.1 in.)

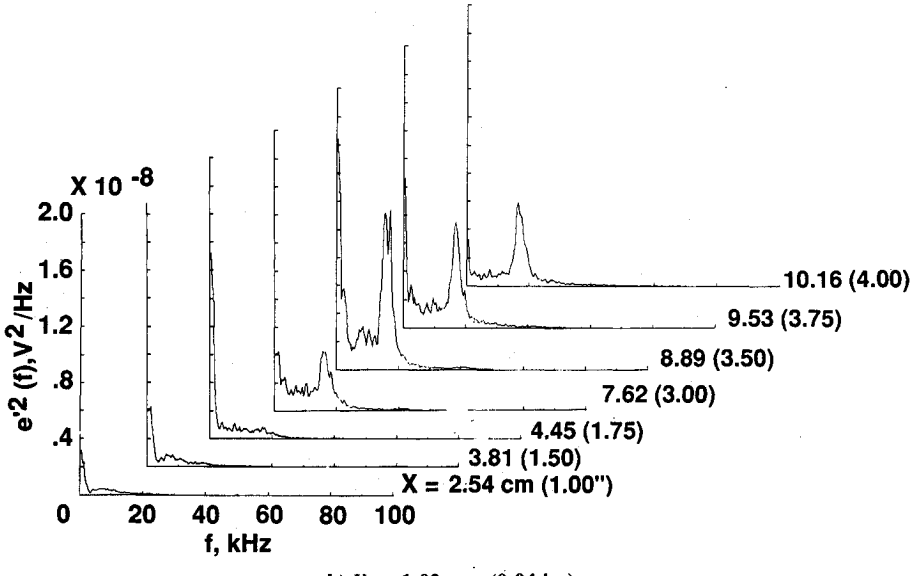

b) Y = 1.02 mm (0.04 in.)

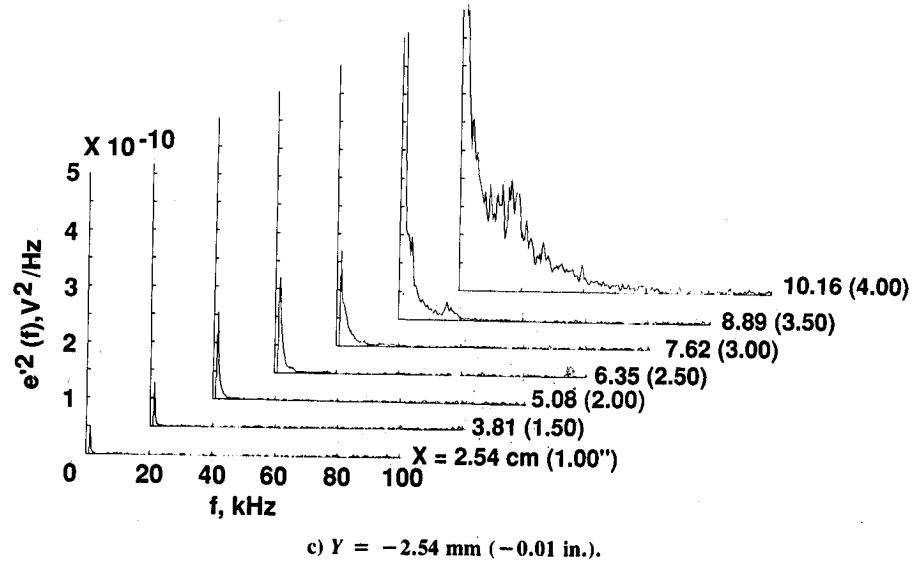

c) Y = −2.54 mm (−0.01 in.).

Fig. 8 Hot-wire power spectra with high $(P'/\bar{P})_{rms}$ at selected X locations; (Re_∞ = 4.33 × 10⁴/cm, M_∞ = 3.5).

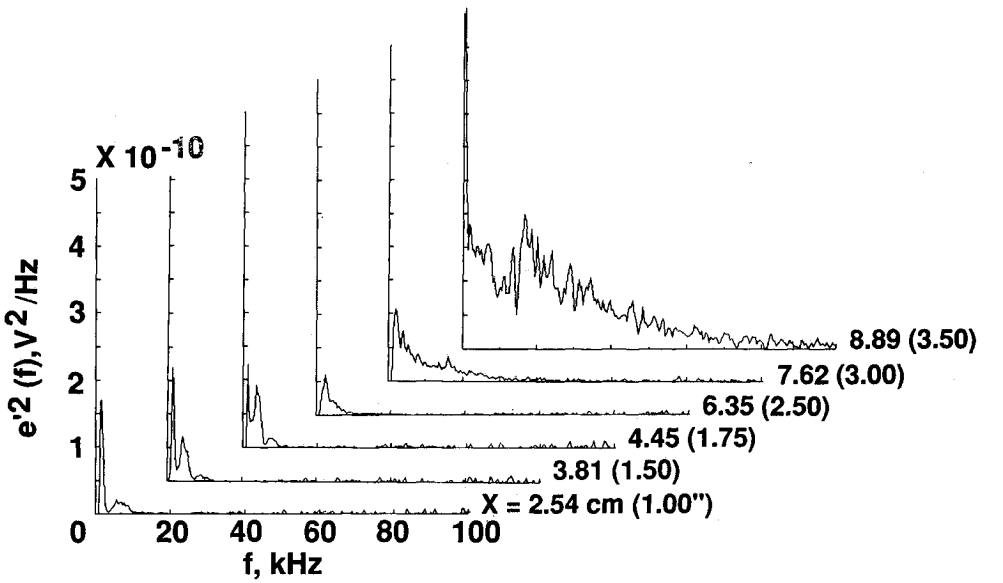

a) Y = 2.54 mm (0.1 in.)

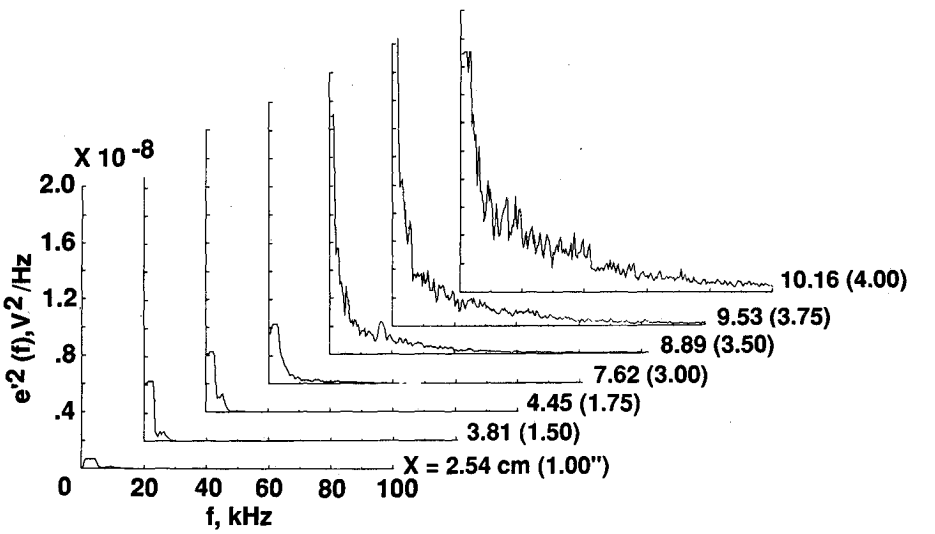

b) Y = 1.02 mm (0.04 in.)

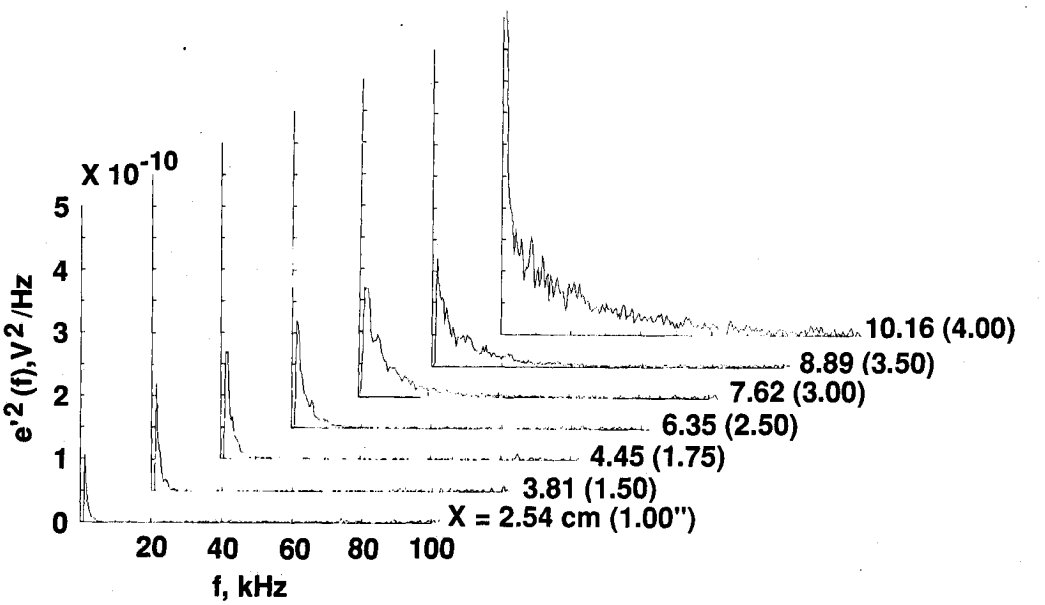

c) Y = −2.54 mm (−0.1 in.).

Fig. 9 Hot-wire power spectra with low $P'/\bar{P})_\infty$ at selected X locations; (Re_∞ = 5.71 × 10⁴/cm, M_∞ = 3.5).

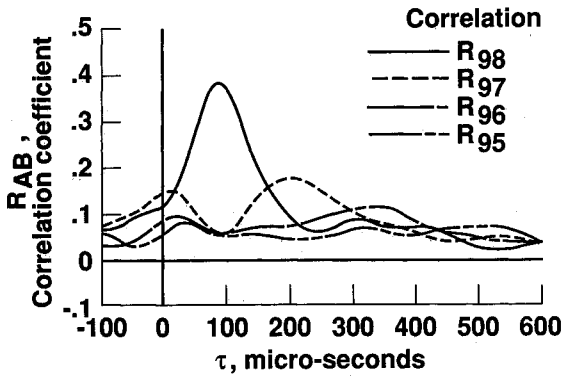

Fig. 10 Two-point correlations referenced to sensor 9; M_∞ = 3.5, Re_∞ = 5.71 × 10^4/cm, low $(P'/\bar{P})_\infty$.

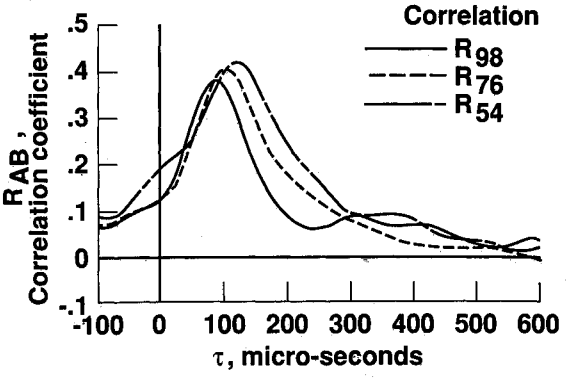

Fig. 11 Two-point correlations between adjacent sensors; M_∞ = 3.5, Re_∞ = 5.71 × 10^4/cm, low $(P'/\bar{P})_\infty$.

shown in Fig. 11. The peaks that corresponded to large τ values are slow-moving disturbances and those that corresponded to small τ values are fast-moving disturbances.

The average convection speed of a disturbance was taken to be the ratio of the separation distance of the sensors to the time delay at the peak of the correlation curve. Note that the rightmost peaks of the correlation curves corresponded to positive τ values, which implies that the slow-moving disturbances were indeed propagating upstream. The average convection speeds U_R of the slow-moving disturbances were between 7.2% ($U_R \simeq$ 46.9 m/s [154 ft/s]) and 11.5% ($U_R \simeq$ 74.7 m/s [245 ft/s]) of the freestream velocity (see Figs. 10 and 11). Preliminary finite-difference solutions of the Navier-Stokes equation (done by Balu Sekar, NASA Langley) predicted a reverse velocity between about 2.4 and 7.3% of the freestream velocity. The finite-difference solutions also predicted an increase in U_R as the distance X increased. This same trend was observed in the hot-film results and is illustrated in Fig. 11 with a shift to the left of the peaks of the correlation curves as X is increased.

3. *Discussion*

Predictions from (temporal) linear stability theory[16] for a confined shear layer at Mach 3.5 indicate that the most unstable frequencies are in excess of 100 kHz. The present data, with or without freestream acoustic fields, indicated wideband growth at lower frequencies; i.e., the shear-layer transition process in the present case is evidently forced by a low-frequency disturbance field not connected with either the freestream acoustic field or linear amplification.

The origin of the 16 kHz spike for the high-noise case has not been resolved. One speculation is that low-frequency disturbances, which are "pumped" by the freestream acoustic field, excite the shear layer for the high-noise case. The initial amplitudes at these critical frequencies may be too small to excite the shear layer for the low-noise case. A nonlinear stability theory that incorporates the influence of the initial disturbance field may be required to resolve this issue.

One interpretation of the present hot-film data is that vorticity and/or entropy waves with frequencies on the order of U_R/δ_L ($\delta_L \sim$ 7.62 mm) are being convected by the recirculating flow from the (dynamic) transitional/turbulent shear-layer impingement/reattachment process upstream into the shear-layer transition regime (see Fig. 12). The frequency of these waves appear as part of the measured disturbance growth in the cavity shear layer. In the opinion of the present authors, there is a high probability that higher frequency acoustic disturbances, with frequencies (on the order of a_2/δ_L) higher than the response characteristics of the thin films used in the present study, were also present; i.e., we expect that the dynamic shear layer reattachment process will generate both vorticity/entropy and acoustic waves that then feed upstream in the subsonic portion of the recirculating flow and dominate the transition process for such (low-speed recirculating flow-

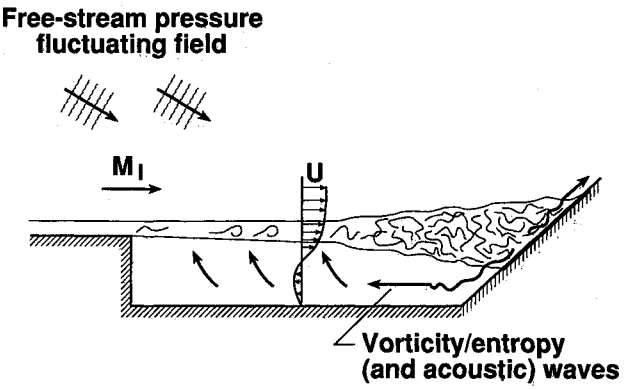

Fig. 12 Transition physics indication from present experiment.

bounded) shear layers (Fig. 12). The expected frequency band of such acoustic waves is also present in the observed shear-layer-amplified disturbance fields. Therefore, for the case where the high-speed free-shear layer is accompanied by an adjacent subsonic recirculating zone that contains a source of either vorticity/entropy or acoustic disturbances, such disturbances can evidently dominate the high-speed shear-layer transition process. The presence of the adjacent wall may also have an important role in the transition process for the shear layer investigated herein. The present observation of the relative insensitivity of shear-layer transition to freestream acoustic fields is consistent with this conclusion.

Concluding Remarks

Free-shear layer transition behavior above a cavity with and without freestream acoustic disturbances was investigated at Mach 3.5. The values of Re_{T_r} obtained, 3.63 × $10^5 < Re_{T_r} <$ 5.30 × 10^5, are in good agreement with previous (conventional, high-noise facility) results. The plot of available free-shear layer transition data (Fig. 7) indicates an increase of Re_{T_r} by more than an order of magnitude between M_1 = 1 and 6, the usual operating range of scramjet combustors. The present study indicates that the transition Reynolds number was not affected (to first order) by the freestream acoustic field. Upstream convected disturbances, believed to be vorticity/entropy waves from the (dynamic) shear-layer impingement/reattachment process, were found to be present in the subsonic recirculating flow of the cavity. Upstream convected disturbances (both acoustic and vorticity/entropy) are believed to be responsible for the insensitivity of Re_{T_r} to the (low-to-moderate) freestream acoustic field; i.e., the high-speed cavity shear-layer transition process is evidently dominated by cavity-flow-induced, as opposed to freestream-induced, disturbance fields. Therefore, for cases where the supersonic free-shear layer is accompanied by an adjacent subsonic recirculating zone that contains a disturbance source (vorticity, entropy, or acoustic), such disturbance can evidently dominate the high-speed shear-layer transition process.

References

[1]Matsuo, K., Aoki, T., and Hirahara, H., "Visual Studies of Characteristics of Slip Stream in Mach Reflection of a Shock Wave," *Proceedings of the Fourth International Symposium on Flow Visualization*, Hemisphere Publishing Corporation, Washington/New York/London, Aug. 1986, pp. 543–548.

[2]Papamoschou, D., and Roshko, A., "Observations of Supersonic Free Shear Layers," AIAA Paper 86-0162, Jan. 1986.

[3]Bogdanoff, D. W., "Compressibility Effects in Turbulent Shear Layers," *AIAA Journal*, Vol. 21, No. 6, June 1983, pp. 926–927.

[4]Ikawa, H., and Kubota, T., "Investigation of Supersonic Turbulent Mixing Layer with Zero Pressure Gradient," *AIAA Journal*, Vol. 13, No. 5, May 1975, pp. 566–572.

[5]Samimy, M., and Elliott, G. S., "Effects of Compressibility on the Structure of Free Shear Layers," AIAA Paper 88-3054A, July 1988.

[6]Ragab, S. A., and Wu, J. L., "Instabilities in the Free Shear Layer Formed by Two Supersonic Streams," AIAA Paper 88-0038, Jan. 1988.

[7]Gropengiesser, H., "Study on the Stability of Boundary Layers and Compressible Fluids," NASA Technical Translation, NASA TT F-12,786, Feb. 1970.

[8]Balsa, T. F., and Goldstein, M. E., "On the Instabilities of Supersonic Mixing Layers, A High Mach Number Asymptotic Theory," *Journal of Fluid Mechanics* (submitted for publication).

[9]Jackson, T L., and Grosch, C. E., "Spatial Stability of a Compressible Mixing Layer," NASA Contractor Report 181671, June 1988.

[10]Chapman, D. R., Kuehn, D. M., and Larson, H. K., "Investigation of Separated Flows in Supersonic and Subsonic Streams with Emphasis on the Effect of Transition," NACA Report No. 1356, 1958.

[11]Gilreath, H. E., and Schetz, J. A., "Transition and Mixing in the Shear Layer Produced by Tangential Injection in Supersonic Flow," American Society of Mechanical Engineers, New York, ASME Paper No. 71-FE-24, Feb. 1971.

[12]Larson, H. K., and Keating, S. J., Jr., "Transition Reynolds Numbers of Separated Flows at Supersonic Speeds," NASA TN D-349, Dec. 1960.

[13]Crawford, D. H., "Investigation of the Flow Over a Spiked-Nose Hemisphere-Cylinder at a Mach Number of 6.8," NASA TN D-118, Dec. 1959.

[14]Tam, C. K. W., and Hu, F. Q., "Instabilities of Supersonic Mixing Layers Inside a Rectangular Channel," AIAA Paper 88-3675, July 1988.

[15]Mack, L. M., "On the Inviscid Acoustic-Mode Instability of Supersonic Shear Flows," Fourth Symposium on Numerical and Physical Aspects of Aerodynamic Flows, California State Univ., Long Beach, CA, Jan. 1989.

[16]Macaraeg, M. G., and Streett, C. L., "New Instability Modes for Bounded, Free Shear Flows," *Physics of Fluids* (to be published).

[17]Beckwith, I. E., Creel, T. R., Jr., Chen, F.-J., and Kendall, J. M., "Free-Stream Noise and Transition Measurements on a Cone in a Mach 3.5 Pilot Quiet Tunnel," NASA TP-2180, Sept. 1983 (also AIAA Paper 83-0042, Jan. 1983).

[18]Hayakawa, K., Smits, A. J., and Bogdonoff, S. M., "Turbulence Measurements in a Compressible Reattaching Shear Layer," *AIAA Journal*, Vol. 22, No. 7, July 1984, pp. 889–895.

[19]Pate, S. R., and Schueler, C. J., "Radiated Aerodynamic Noise Effects on Boundary-Layer Transition in Supersonic and Hypersonic Wind Tunnels," *AIAA Journal*, Vol. 7, No. 3, March 1969, pp. 450–457.

[20]Pate, S. R., "Dominance of Radiated Aerodynamic Noise on Boundary-Layer Transition in Supersonic-Hypersonic Wind Tunnels—Theory and Applications," Arnold Engineering Development Center, Arnold Air Force Station, Tennessee, AEDC TR-77-107, March 1978.

[21]Morkovin, M. V., "Transition at Hypersonic Speeds," NASA Contractor Report 178315, May 1987.

[22]Laufer, J., "Aerodynamic Noise in Supersonic Wind Tunnels," *Journal of Aerospace Science*, Vol. 28, No. 9, Sept. 1961, pp. 685–692.

[23]King, R. A., Creel, T. R., Jr., and Bushnell, D. M., "Experimental Study of Free-Shear Layer Transition Above a Cavity at Mach 3.5," AIAA Paper 89-1813, June 1989.

[24]Hama, F. R., "Experimental Investigations of Wedge Base Pressure and Lip Shock," NASA Report No. 32-1033, Dec. 1966.

[25]Demetriades, A., "Transition to Turbulence in Free Shear Layers," Air Force Office of Scientific Research, Bolling Air Force Base, Washington, DC, AFOSR-TR-80-0056, Oct. 1979.

[26]Birch, S. F., and Keyes, J. W., "Transition in Compressible Free Shear Layers," *Journal of Spacecraft and Rockets*, Vol. 9, No. 8, Aug. 1972, pp. 623–624.

[27]Kavanau, L. L., "Results of Some Base Pressure Experiments at Intermediate Reynolds Numbers with $M = 2.84$," Institute of Engineering Research, Univ. of California, Berkeley, CA, Report No. He-150-117, Oct. 1953.

[28]Reller, J. O., Jr., and Hamaker, F. M., "An Experimental Investigation of the Base Pressure Characteristics of Nonlifting Bodies of Revolution at Mach Numbers from 2.73 to 4.98," NACA TN-3393, Mar. 1955.

[29]Sato, H., "Experimental Investigation on the Transition of Laminar Separated Layer," *Journal of the Physical Society of Japan*, Vol. 11, No. 6, June 1956, pp. 702–709.

[30]Emami, S., Morrison, G., and Tatterson, G., "Eddy Viscosity Distributions Through the Transition of an Incompressible Free Jet," *Journal of Fluids Engineering*, Vol. 110, March 1988, pp. 98–100.

[31]Brower, T., "Experiments on the Free Shear Layer Between Adjacent Supersonic Streams," M.S. Thesis, Montana State University, Bozeman, MT., March 1983.

[32]Papamoschou, D., "Experimental Investigation of Heterogeneous Compressible Shear Layers," Ph.D. Dissertation, CALTECH, Pasadena, CA, 1986.

[33]Edney, B., "Anomalous Heat Transfer and Pressure Distributions on Blunt Bodies at Hypersonic Speeds in the Presence of an Impinging Shock," The Aeronautical Research Institute of Sweden, Stockholm, Sweden, FFA Report 115, Feb. 1968.

[34]Wusk, M. S., Carraway, D. L., and Holmes, B. J., "An Arrayed Hot-Film Sensor for Detection of Laminar Boundary-Layer Flow Disturbance Spatial Characteristics," AIAA Paper 88-4677-CP, Sept. 1988.